SUPPORTING INFORMATION

Simple and Efficient Separation of Atomically Precise Noble Metal Clusters

Atanu Ghosh,[†,‡] Jukka Hassinen, [§,‡] Petri Pulkkinen,[#] Heikki Tenhu,[#] Robin H. A. Ras[§,*] and Thalappil Pradeep[†,*]

[†] DST Unit of Nanoscience (DST UNS) and Thematic Unit of Excellence (TUE), Department of Chemistry, Indian Institute of Technology Madras, Chennai 600 036, India.

[§] Department of Applied Physics, Aalto University (Helsinki University of Technology), Puumiehenkuja 2, FI-02150 Espoo, Finland.

[#] Department of Chemistry, University of Helsinki, P.O. Box 55, 00014 Helsinki, Finland.

‡ These authors contributed equally.

* robin.ras@aalto.fi (fax: +358-9-47023155), pradeep@iitm.ac.in (fax: +91-44-2257 0509/0545)

Content

1. Separation of BT and PET Protected Au_{25}

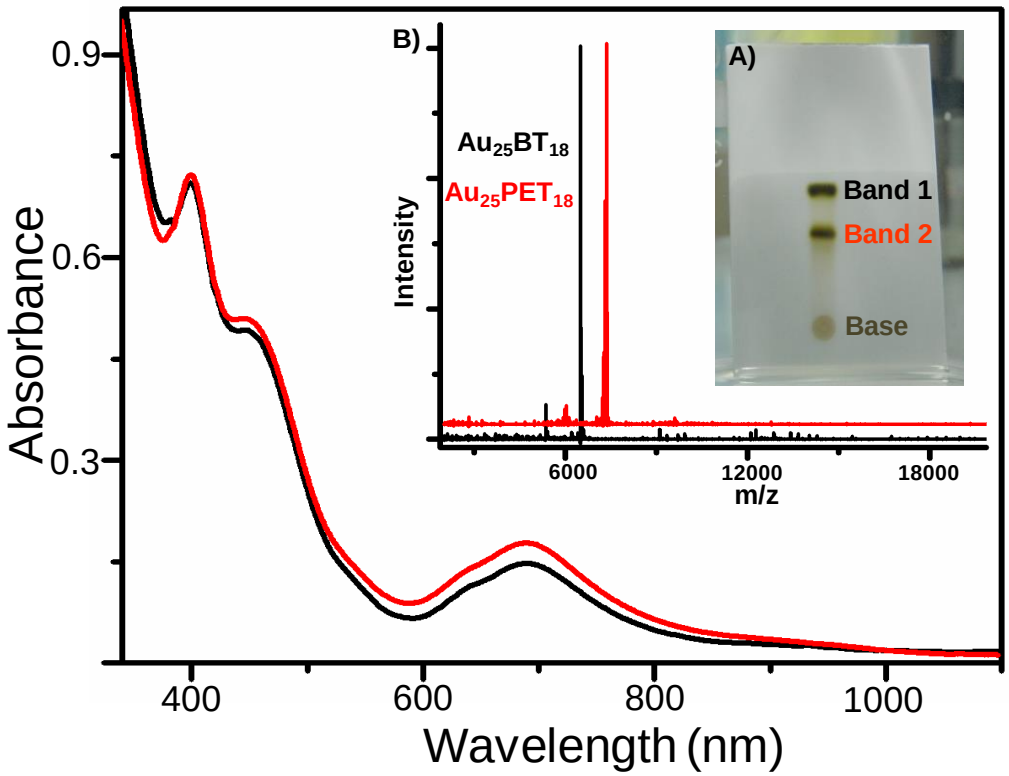

Figure S-1. UV-vis spectra of TLC separated materials. A) Photograph of the TLC plate used for cluster separation. Bands 1 and 2 are due to two separated clusters. B) MALDI MS data of TLC separated materials confirming that bands 1 (black trace) and 2 (red trace) are pure $Au_{25}BT_{18}$ and $Au_{25}PET_{18}$, respectively.

2. Oxidation of $Au_{25}PET_{18}^-$ During a TLC Run

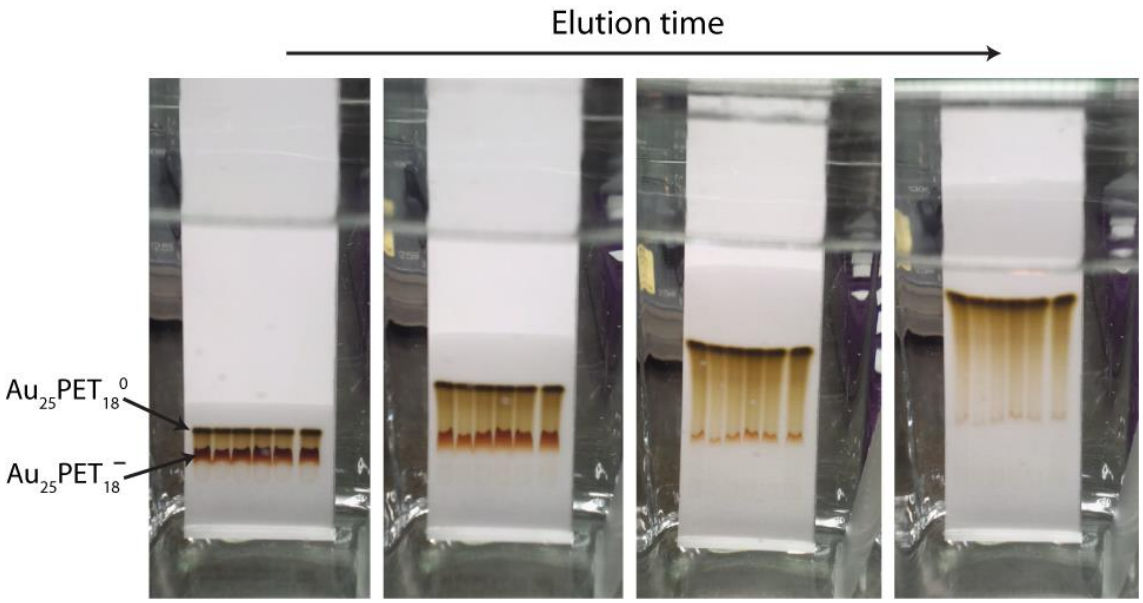

Figure S-2. Oxidation of $Au_{25}PET_{18}^-$ to $Au_{25}PET_{18}^0$ during the TLC run (DCM/hexane 60:40). The clusters were spotted directly after the synthesis of $Au_{25}PET_{18}$ in order to prevent oxidation during storage. However, we observed the presence of both oxidation states already in the beginning of the TLC run. During elution, the lower band ($Au_{25}PET_{18}^-$) gradually converts to $Au_{25}PET_{18}^0$ and causes a tail to the upper band.

3. TLC Separation of $Au_{25}PET_{18}^{-}$ and $Au_{25}PET_{18}^{0}$

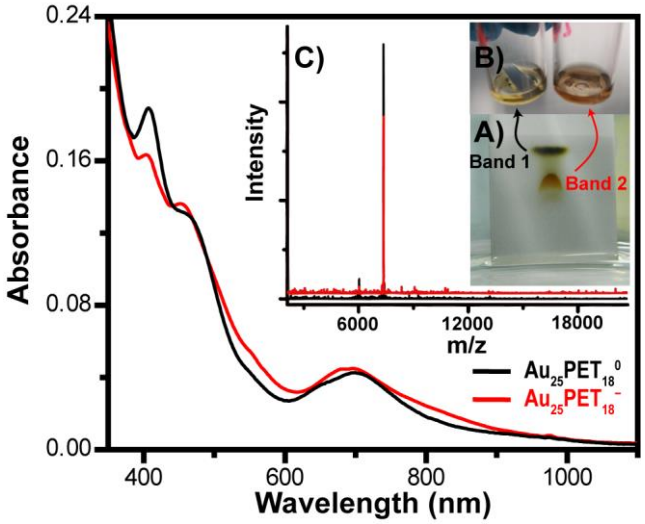

Figure S-3. UV-vis spectra of the TLC separated $Au_{25}PET_{18}^{0}$ and $Au_{25}PET_{18}^{-}$. A) Photograph of the TLC plate used for cluster separation (DCM/hexane 70:30). Bands 1 and 2 are due to two separated clusters. B) Photograph of the extracted clusters showing the visible color difference between the two charge states of $Au_{25}PET_{18}$. C) MALDI MS data of TLC separated materials confirming that bands 1 (black trace) and 2 (red trace) are pure $Au_{25}PET_{18}^{0}$ and $Au_{25}PET_{18}^{-}$, respectively.

4. Retention Factors for All Separated Clusters

Table S-1. TLC Eluent Compositions and R_f Values of All Separated Clusters

Figure	Eluent (DCM/Hexane)	Separated Clusters*	R_f Value
1	40:60	$Au_{25}HT_{18}$	0.89
		$Au_{25}BT_{18}$	0.77
2	60:40	$Au_{25}PET_{18}$	0.65
		$Au_{144}PET_{60}$	0.44
4	30:70	$Au_{25}BT_{18}$	0.33
		$Au_{25}Calix_1BT_{16}$	0.14
		$Au_{25}Calix_1BT_{14}$	0.09
		$Au_{25}Calix_2BT_{10\text{-}16}$	0.04
5	35:65	$Au_{25}Calix_2BT_{12\text{-}14}$	0.19
		$Au_{25}Calix_2BT_{10\text{-}12}$	0.11
		$Au_{25}Calix_{2\text{-}4}BT_{6\text{-}12}$	0.06
S-1	60:40	$Au_{25}BT_{18}$	0.88
		$Au_{25}PET_{18}$	0.62
S-3	70:30	$Au_{25}PET_{18}$	0.73
		$Au_{25}PET_{18}^-$	0.58

* Unless otherwise noted, the clusters have a neutral core charge.

5. Peak Positions and Assigned Compositions of $Au_{25}Calix_{0\text{-}3}BT_{6\text{-}18}$

Table S-2. Compositions Observed in MALDI MS of $Au_{25}Calix_{0\text{-}3}BT_{6\text{-}18}$: Experimental and Theoretical m/z Values

Peak ID	Composition	*m/z*		Difference*
		Exp.	Theor.	
1	$Au_{25}BT_{18}$	6506.0	6528.9	22.9
2	$Au_{25}Calix_1BT_{14}$	6919.1	6945.0	25.9
3	$Au_{25}Calix_1BT_{16}$	7098.0	7123.1	25.1
4	$Au_{25}Calix_1BT_{18}$	7274.8	7301.5	26.7
5	$Au_{25}Calix_2BT_{10}$	7335.5	7361.2	25.7
6	$Au_{25}Calix_2BT_{12}$	7512.8	7539.2	26.4
7	$Au_{25}Calix_2BT_{14}$	7691.1	7718.2	27.1
8	$Au_{25}Calix_2BT_{16}$	7868.6	7896.6	28.0
9	$Au_{25}Calix_3BT_6$	7747.8	7777.0	29.2
10	$Au_{25}Calix_3BT_8$	7925.3	7955.3	30.0
11	$Au_{25}Calix_3BT_{10}$	8104.9	8134.4	29.5
12	$Au_{25}Calix_3BT_{12}$	8281.1	8312.8	31.7
13	$Au_{25}Calix_3BT_{14}$	8459.8	8491.2	31.4

* Difference increases in a linear fashion indicating that the difference originates from slight inaccuracy in mass calibration. However, the peak pattern in MALDI MS closely resembles the pattern observed in ESI MS from a similar sample,[1] thus confirming the interpretation.

Table S-3. Interpretations of Ligands' Binding Modes on $Au_{25}Calix_{0\text{-}3}BT_{6\text{-}18}$ Clusters

Composition	Number of Calix		BT bound to Au
	Tetradentate	Bidentate	
$Au_{25}BT_{18}$	0	0	18
$Au_{25}Calix_1BT_{14}$	1	0	14
$Au_{25}Calix_1BT_{16}$	0	1	16
$Au_{25}Calix_1BT_{18}$	0	1	16 [a]
$Au_{25}Calix_2BT_{10}$	2	0	10
$Au_{25}Calix_2BT_{12}$	1	1	12
$Au_{25}Calix_2BT_{14}$	0	2	14
$Au_{25}Calix_2BT_{16}$	0	2	14 [a]
$Au_{25}Calix_3BT_6$	3	0	6
$Au_{25}Calix_3BT_8$	2	1	8
$Au_{25}Calix_3BT_{10}$	1	2	10
$Au_{25}Calix_3BT_{12}$	0	3	12
$Au_{25}Calix_3BT_{14}$	0	3	12 [a]

[a] Two BT are presumed to bind to Au-bound Calix with disulfide bridges.

6. Sticking of Clusters to TLC Plate Demonstrated

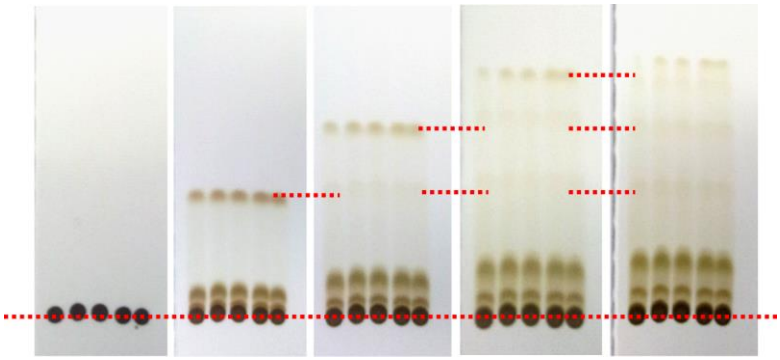

Figure S-4. TLC separation of $Au_{25}Calix_{0\text{-}3}BT_{6\text{-}18}$ clusters: photographs of the same TLC plate between runs showing slight sticking of the first band. Eluent used in the separation was DCM/hexane 30:70.

7. Monitoring the Progress of Cluster Synthesis Using TLC

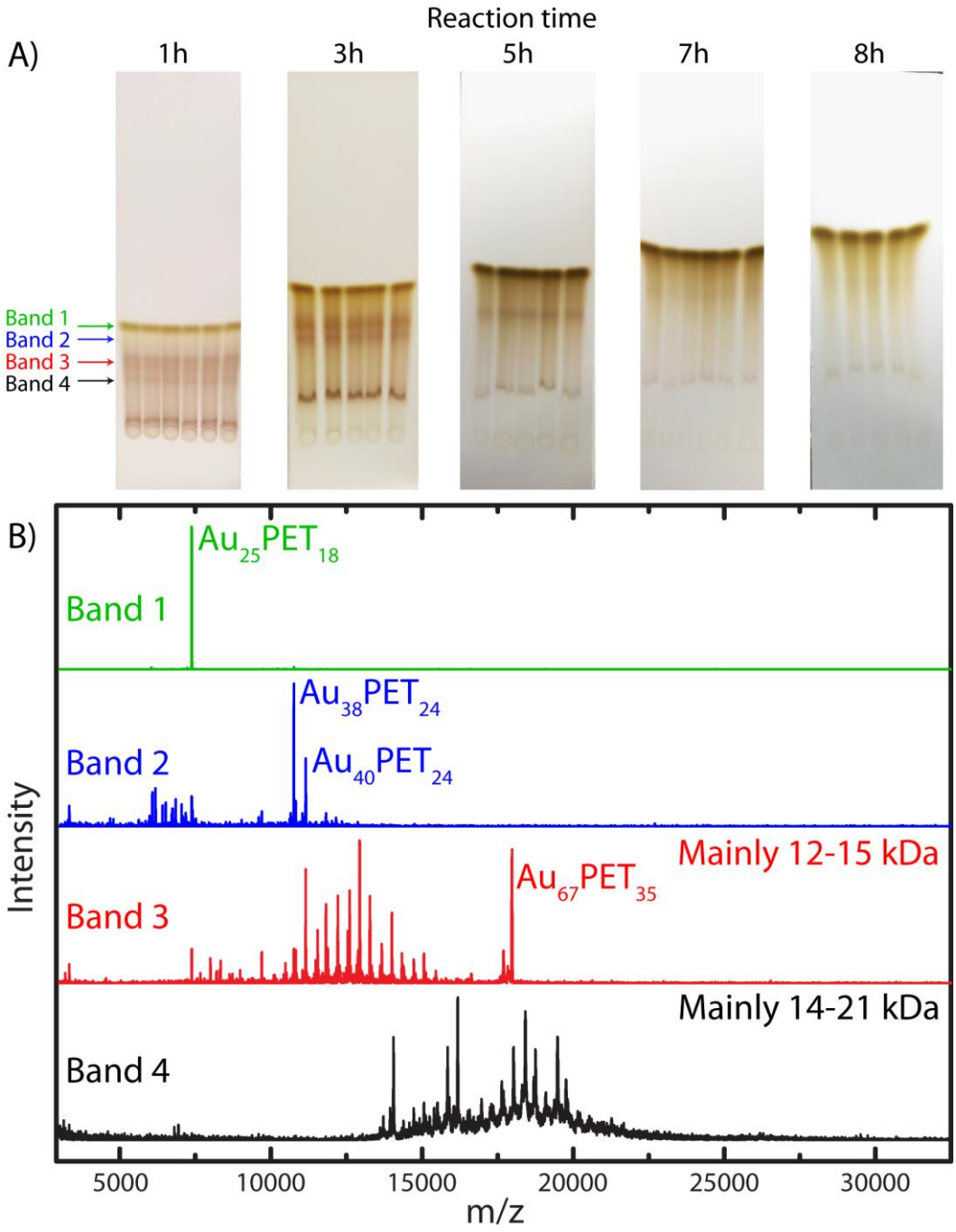

Figure S-5. A) Photographs of $Au_{25}PET_{18}$ synthesis monitored by TLC (DCM/hexane 60:40). The relative amount of $Au_{25}PET_{18}$ clusters increases with time, whereas larger clusters disappear. B) MALDI MS data of bands 1–4 after 1 h of reaction. Band 1 is composed of pure $Au_{25}PET_{18}$ clusters (obs. 7380 m/z, theor. 7391 m/z) and band 2 is a mixture of $Au_{38}PET_{24}$ and $Au_{40}PET_{24}$, which are known, stable compositions (obs. 10759 and 11152 m/z, theor. 10774 and 11168 m/z, respectively).[3] Bands 3 and 4 are composed of multiple larger clusters. In addition, band 3 shows a signal separate from the main pattern, which is interpreted as $Au_{67}PET_{35}$ (obs. 17975 m/z, theor. 17999 m/z) based on previous reports.[4] In general, the data implies a correlation between the size and the retention factor of clusters protected with the same ligand.

8. References

1. Hassinen, J.; Pulkkinen, P.; Kalenius, E.; Pradeep, T.; Tenhu, H.; Häkkinen, H.; Ras, R. H. A. *J. Phys. Chem. Lett.* **2014**, *5*, 585−589.
2. Qian, H.; Jin, R. *Chem. Mater*. **2011**, *23*, 2209−2217.
3. Knoppe, S.; Dharmaratne, A. C.; Schreiner, E.; Dass, A.; Bürgi, T. *J. Am. Chem. Soc.* **2010**, *132*, 16783–16789.
4. Nimmala, P. R.; Yoon, B.; Whetten, R. L.; Landman, U.; Dass, A. *J. Phys. Chem. A* **2013**, *117*, 504−517.